Effect of Gramicidin A on Structure and Dynamics of Lipid Vesicle Bilayers. A Time-Resolved Fluorescence Depolarization Study†

Johan M. Muller,* Gijsbert van Ginkel, and Ernst E. van Faassen

Debye Research Institute and Department of Molecular Biophysics, Buijs Ballot Laboratory, University of Utrecht, Princetonplein 5, 3584 CC Utrecht, The Netherlands

Received August 26, 1994; Revised Manuscript Received November 16, 1994⊗

ABSTRACT: We investigated the effects of the hydrophobic small peptide antibiotic gramicidin A (gA) on the properties of vesicle bilayers in the liquid crystalline state. Time-resolved fluorescence anisotropy experiments were performed with unilamellar vesicles of the lipids DMPC, POPC, DOPC, EGGPC, DLPC, DOPG, and SQDG containing various concentrations of gA in two different conformations using TMA-DPH and DPHPC as fluorescent probes. These analogues of DPH were taken to study the gA induced change in the structural and dynamical properties of the lipid bilayer in different portions of the hydrophobic region. The time-resolved anisotropy data were analyzed using the recently introduced compound motion model [van der Sijs, D. A., et al. (1993) *Chem. Phys. Lett. 216*, 559; Muller, J. M., et al. (1994) *Chem. Phys. 185*, 393]. In general, gA raises the order and reduces the rotational diffusion coefficient for the probes in the bilayer. In DOPC vesicles this ordering effect of gA on the bilayer is found to depend on both the conformation of the peptide and the depth in the bilayer at which the order is probed. This significant effect of gA conformation on the lipid order parameter profile suggests that the shape of the gA dimer in the bilayer, which is determined by its conformation, affects the order of the adjacent DOPC lipid acyl chains.

Gramicidin A (gA)[1] is currently the best studied example of a channel-forming peptide, and together with melittin it is among the best characterized peptide antibiotics and lytic agents. Various aspects of gramicidin and its effects have been widely studied with different techniques: the role of its conformation in the conducting state, the kinetics of the cation transport through gramicidin channels, and the effect of gA on the supporting lipid membrane. Gramicidin was found to be an effective promotor of inverted hexagonal H_{II} phase formation in various synthetic model and biological membranes. It has been shown that the presence of the four bulky tryptophan amino residues near the C-terminal is crucial to this phase modulating ability [for reviews, see Andersen (1984), Urry (1985), Killian and de Kruijff (1986), Cornell (1987), Wallace (1990), Andersen et al. (1992), and Killian (1992)].

Because of its ability to form conducting cation-selective transmembrane channels, its exceptionally strong effect on macroscopic lipid organization, and the relative ease with which this oligopeptide is handled experimentally, gA has become a prototype for studies of protein−lipid model systems. Its primary structure is linear and consists of only 15 amino acid residues which have alternate L and D chirality. gA is a member of a large family of polypeptide antibiotics produced by *Bacillus brevis*, an aerobic soil bacterium. The sequence of gA from N- to C-terminal is formyl-LVal_1-Gly_2-LAla_3-DLeu_4-LAla_5-DVal_6-LVal_7-DVal_8-LTrp_9-DLeu_{10}-LTrp_{11}-DLeu_{12}-LTrp_{13}-DLeu_{14}-LTrp_{15}-ethanolamine. The natural mixture of gramicidins is denoted as gramicidin D, the main and most active constituent of which is gA. Because of the absence of either charged or hydrophilic side chains and its blocked termini, gA is almost insoluble in water and incorporates easily in the hydrophobic region of phospholipid membranes. This is why gramicidin can be utilized as a model for the membrane-spanning part of intrinsic membrane proteins. In this paper we study the effect of gA on the molecular orientational order and reorientational dynamics of the lipid molecules in vesicle membrane bilayers.

Due to its small size and its lack of extensive tertiary structure, gA can occur in very different conformations, depending on the organic solvent or other details of its environment. In phospholipid membranes conformations of the peptide may be distinguished according to their ability to form cation permeable transmembrane channels. The so-called channel conformation has been shown to be a right-handed head-to-head single-stranded helical dimer consisting of two gramicidin molecules, i.e., the monomer helices are associated with each other at the N-terminals; in consequence, the tryptophan residues reside near the water interface of the bilayer. The gramicidin monomers in this

† This work was supported by a research grant to J.M.M. from the Stichting voor Biofysica (Foundation for Biophysics) under the auspices of NWO (Netherlands Organization for Scientific Research).

* Corresponding author.

⊗ Abstract published in *Advance ACS Abstracts,* February 1, 1995.

[1] Abbreviations: BRD, Brownian rotational diffusion; CD, circular dichroism; CMM, compound motion model; DLPC, dilineoylphosphatidylcholine; DMPC, dimyristoylphosphatidylcholine; DMSO, dimethyl sulfoxide; DOPC, dioleoylphosphatidylcholine; DOPG, dioleoylphosphatidylglycerol; DPH, diphenylhexatriene; DPHPC, ((diphenylhexatrienyl)propanoyl)palmitoylphosphatidylcholine; DPPC, dipalmitoylphosphatidylcholine; DSC, differential scanning calorimetry; EGGPC, egg yolk phosphatidylcholine; ESR, electron spin resonance; ETOH, ethanol; gA, gramicidin A; HPLC, high-performance liquid chromatography; HPTLC, high-performance thin layer liquid chromatography; IR, infrared; NMR, nuclear magnetic resonance spectroscopy; PC, phosphatidylcholine; PG, phosphatidylglycerol; POPC, palmitoyloleoylphosphatidylcholine; POPE, palmitoyloleoylphosphatidylethanolamine; SCIC, strong collision in cone; SQDG, sulfoquinovosyldiacylglycerol; TFE, 2,2,2-trifluoroethanol; TMA-DPH, (trimethylammonium)diphenylhexatriene.

0006-2960/95/0434-3092$09.00/0

β-type helical dimer each have 6.3 residues per turn and a central hole of 4 Å in diameter, while the total length of the dimer amounts to 25−30 Å, thus allowing it to span a lipid bilayer. The peptide backbone is stabilized by alternating interchain hydrogen bonds from amide and formyl groups of both gramicidin molecules in the dimer. Due to their alternating chirality, the hydrophobic amino residues are oriented to the exterior of the helix, while the carbonyl groups line the hydrophilic inside of the gramicidin channel. When gramicidin is incorporated in a lipid bilayer, the hydrophobic amino acid side chains are buried in the surrounding acyl-chain region of the bilayer. The channel conformation state has been proved to be the energetically most stable and thus the equilibrium state of the gramicidin dimer (Bañó et al., 1989, 1991).

Besides this channel conformation, alternative conformations of gA have been identified that do not form ion-transporting transmembrane channels in phospholipid membranes, e.g., the double-stranded antiparallel conformation. Although these have been shown to occur in more than one variety (Veatch & Blout, 1974; Killian, 1992), they are here collectively referred to as the "nonchannel conformation" in the following. This nonchannel conformation is to be regarded as a metastable state: by prolonged heat incubation it can be converted into the channel conformation (Killian & Urry, 1988). The channel and nonchannel conformations distinguish themselves not only with respect to the ion-transport capacity but also by their geometrical shape. The former is reported to be diabolo-shaped, while the latter has a more cylindrical form. These observations lead us to expect that differences in their effect on the surrounding lipid matrix, if any, will show up in the depth of the bilayer. Therefore a suitable experimental method should provide selectivity as to the part of the bilayer probed. Such a method could employ for instance deuterium NMR for selectively deuterated lipids or fluorescence techniques with probes at various depth in the bilayer as is done in this paper.

Indeed, it has been shown that the channel conformation, apart from its conductance of small cations, can also dramatically affect the lipid environment in which gramicidin is embedded. gA has the ability to induce the inverted hexagonal H_{II} lipid phase in, e.g., DOPC or erythrocyte ghosts, but only in its channel conformation (Tournois et al., 1987, 1988). This conformation can be controlled via the solvent from which the peptide is added or cosolubilized. gA adopts either the nonchannel conformation—from ethanolic solution—or the channel conformation as described above—from dimethyl sulfoxide or trifluoroethanol solution (Tournois et al., 1987; Killian & Urry, 1988).

Gramicidin and gA have been the focus of numerous studies during the past 20 years. Using NMR, ESR, DSC, CD, IR and Raman spectroscopy, and X-ray diffraction techniques, gramicidin has been studied and characterized both in solution and embedded in lipid bilayers. A few studies have employed the fluorescence of the intrinsic tryptophans of gramicidin (Haigh et al., 1979; Spisni et al., 1983; Masotti et al., 1986; Scarlata, 1988; Cox et al., 1992; Muller et al., 1989). While this intrinsic fluorescence of gA reflects the behavior of the peptide itself, the effect of this peptide on the surrounding lipids has to be studied using extrinsic lipid-soluble fluorescent probes. Time-resolved fluorescence depolarization experiments on such probes can provide microscopic information on structural and dynamical properties of lipid bilayers (e.g., Best et al., 1987; van Langen et al., 1987, 1989; Wang et al., 1991; Muller et al., 1994a,b).

The aim of the present paper is 3-fold. In the first place, using time-resolved fluorescence probe techniques, we investigate the effects of nonchannel gA in unilamellar vesicles of lipids in the liquid crystalline state of varying chain length, unsaturation, and headgroup.

Secondly, in DOPC vesicles a direct comparison is made between the effects due to channel and nonchannel conformations of gA. As motivated above, distinction should be made between surface and inner parts of the bilayer. Therefore we employed two particular probes, TMA-DPH and DPHPC, which have their fluorescent DPH moieties located near the bilayer surface and in the hydrophobic region respectively.

In the third place, we apply the compound motion model (CMM) for the time-resolved fluorescence anisotropy for the first time as a method for the study of peptide−lipid interactions. This novel model was introduced recently because it lacks certain drawbacks (van der Sijs et al., 1993) associated with the well-known Brownian rotational diffusion and wobble-in-cone models. Previously, this model has been applied to analyze data from single-component lipid vesicle systems (Muller et al., 1994a,b). Here the work is extended to the situation where a peptide is incorporated in the bilayer. We note that for vesicles it is essential that the fluorescence anisotropy experiments are time-resolved, as steady-state results cannot disentangle the intertwined effects of orientational order and reorientational dynamics of the probes.

Our main results are the following. The CMM is shown to be a fruitful model to investigate peptide−lipid interactions. In general, gA raises the order and reduces the rotational diffusion coefficient for the probes in the vesicle bilayers studied. In DOPC vesicles, gA enhances the lipid order in a depth-dependent way as monitored with TMA-DPH and DPHPC. Moreover, the perturbation of the bilayer structure depends slightly on the conformation of gA (i.e., channel or nonchannel). This conformational effect of gA on the lipid order parameter profile suggests that it is the shape of the gA dimer in the bilayer, determined by its conformation, which affects the order of the adjacent DOPC lipid molecules.

MATERIALS AND METHODS

Materials. The phospholipids dimyristoyl(14:0,14:0)-phosphatidylcholine (DMPC), palmitoyl-Δ^9-oleoyl(16:0,18:1)phosphatidylcholine (POPC), Δ^9dioleoyl (18:1,18:1) phosphatidylcholine DOPC), $\Delta^{9,12}$-dilineoyl(18:2,18:2)phosphatidylcholine (DLPC), Δ^9-dioleoyl(18:1,18:1)phosphatidylglycerol (DOPG), and egg yolk phosphatidylcholine (EGGPC) and the sulfolipid sulfoquinovosyldiacylglycerol (SQDG) were obtained from Lipid Products (Surrey, U.K.) and were checked for purity with TLC (thin layer chromatography). The fluorescent probes TMA-DPH (1-[4-(trimethylammonio)phenyl]-6-phenyl-1,3,5-hexatriene) and DPH-PC (2-(3-(diphenylhexatrienyl)propanoyl)-3-palmitoyl-L-α-phosphatidylcholine) were bought from Fluka AG and Molecular Probes Inc. (Junction City, OR), respectively, and were dissolved in ethanol to prepare stock solutions which were kept in the dark at 4 °C. Gramicidin A was purified by the Centre for Biomembranes and Lipid Enzymology (CBLE), University of Utrecht, The Netherlands, using high-performance liquid chromatography (HPLC) and was a

generous gift from Drs. J. A. Killian, H. Tournois, and T. C. B. Vogt. All chemicals were of analytic grade.

Vesicle Preparation. Unilamellar vesicles of one lipid only were prepared by first dissolving 4 mg of lipid in ethanol. The appropriate amounts from fresh stock solutions of the fluorescent probes TMA-DPH or DPHPC were codissolved in ethanol in order to get a probe to lipid molecular ratio of 1:250.

In concentrated emulsions of most lipids, gA was found in the literature not to induce a H_{II} phase transition in the concentration regime considered here (Killian, 1992). Therefore, we incorporated gA in the nonchannel conformation in our vesicle samples. However, as the effects of gA in a lipid emulsion are expected to be strongest in DOPC (van Echteld et al., 1982; Killian et al., 1987), we selected this lipid to compare the effect of both the channel and nonchannel conformations of gA. These may be achieved by codissolving gA from trifluoroethanol or ethanol solution, respectively. Details of the procedure are given in Tournois et al. (1987) and Killian and Urry (1988). We note that both the strong dilution and the unilamellarity of the vesicles make a transition to H_{II} phase highly improbable according to current models (Killian, 1992). Indeed, it has been shown that gA does not induce a full-scale transition in DOPC vesicles (Cox et al., 1992).

Two stock solutions of gramicidin A in ethanol and in trifluoroethanol were prepared in a molarity of 1 mM; due to the differing dimerization constants of the peptide in the solvents, this means that at this peptide concentration in ethanol dimers are predominant in contrast to trifluoroethanol, where monomers are expected to form the main species (Veatch & Blout, 1974; Killian, 1992). Before gA was added from trifluoroethanol solution to the lipid, it was certified that all traces of ethanol were removed from the lipid sample by prior overnight evaporation under high vacuum. After the resultant lipid/probe/gA mixture was dried under a continuous stream of nitrogen, an aliquot of Tris-EDTA buffer was added, and the sample was vigorously vortexed for 1 min. For the subsequent preparation of the dilute unilamellar vesicle suspensions two different methods were applied. Some samples were sonicated in a bath type sonicator for 15−45 min until a clear suspension resulted. This suspension was then centrifuged at 50000*g* during 1 h in a Sorval RC5 ultracentrifuge, and the supernatant was used for experiments. The other method consisted of extruding the vortexed cloudy lipid/buffer suspension successively through three Nucleopore plastic filters with pores of 600, 200, and 100 nm diameter, respectively, using pressurized nitrogen (Mayer et al., 1986). It was checked for a number of systems containing gA that the fluorescence data did not depend on either method of vesicle preparation employed here. Furthermore, for the cases of DOPC and POPC vesicles the conformation of the incorporated gA was confirmed by circular dichroism measurements on a Jasco J-600 spectrometer. The CD spectra in the wavelength region of 210−260 nm are known to distinguish between channel and nonchannel conformations (Vogt et al., 1991); the CD spectra for DOPC are shown in Figure 1. All clear vesicle suspensions were kept in the dark and at 4 °C as much as possible. The samples were used for measurements within 4 days after preparation. Phospholipid content of the samples was quantified afterwards by phosphorus determination (Chen et al., 1956).

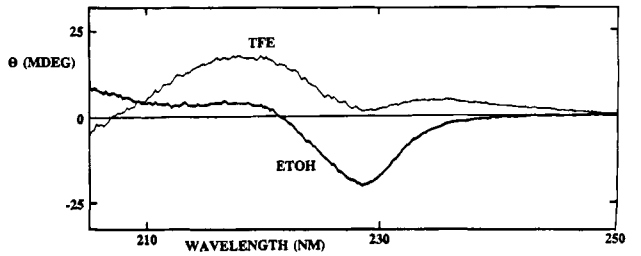

FIGURE 1: Circular dichroism spectra for gramicidin A embedded in sonicated small unilamellar vesicles of DOPC. gA was incorporated from the solvents ETOH and TFE in a peptide/lipid molar ratio of 1:50. The spectra clearly show the difference between both solvent-induced conformations of gA.

Time-Resolved Fluorescence Anisotropy and Lifetime Measurements. The time-resolved fluorescence lifetime and anisotropy measurements were performed with the Synchrotron Radiation Source (SRS) in Daresbury (U.K.) operating in single-bunch mode at a 3 MHz repetition rate with a 250 ps pulse width. The excitation SPEX monochromator setting was at 360 ± 3 nm; in addition a 360 nm interference filter was used for excitation. We note that the optical absorption bands of DPH derivatives like TMA-DPH and DPHPC are well away from those of tryptophan and gramicidin, so that excitation of the intrinsic fluorescence of gramicidin was avoided in our experiments. A 440 nm interference filter and a GG395 cutoff filter defined the fluorescence emission wavelength. We used the standard electronic setup for time-correlated single photon counting as described previously (van Langen et al., 1989). The photomultiplier tube (PMT, Philips XP2020Q) was Peltier cooled down to −20 °C and fed with −2700 V. Correction G-factors for the differential sensitivity to the polarized fluorescence light of the PMT and optics were determined routinely during the experiments and accounted for in the subsequent analysis; the deviation from 1.00 did not exceed 1%. Except for DMPC, all experiments were performed at the ambient room temperature of 20 ± 1 °C; DMPC was studied at 35 °C, well above the phase transition from the gel to the liquid crystalline state. To record complete decay curves within the range of 1022 channels of the multichannel analyzer (MCA), channel widths of 0.040 or 0.080 ns/channel were used; in channels 1023 and 1024 of the MCA the elapsed real and live time of the measurement were stored. Time-resolved anisotropy decays for TMA-DPH were measured using either a 40 or a 80 ps channel width, while the profiles for DPHPC, which has a longer fluorescence lifetime, were recorded at a 80 ps channel width only. For both probes the excitation flash profile was obtained from the elastic scattering of the vesicle sample monitored at the excitation wavelength. In the anisotropy experiments the parallel and perpendicular components of the emitted fluorescence light were collected in an alternating sequence for 25 s each. The count rate was kept at less than 1% of the synchrotron repetition rate of 3 MHz to avoid photon pulse pile-up in the electronics. The optical filter combination was checked and optimized for each sample to minimize elastic scatter.

Compound Motion Model for the Time-Resolved Fluorescence Anisotropy. In the time-resolved fluorescence anisotropy experiments decribed here a sample of lipid vesicles doped with TMA-DPH or DPHPC in aqueous suspension was illuminated by a flash of vertically polarized light to excite the probe; subsequently, the decay of the fluorescence

emission was monitored in both vertically (||) and horizontally ($\perp$) polarized light. The time-dependent intensities of these components can be expressed (Lakowicz, 1986) in terms of the anisotropy decay $r(t)$ and the intrinsic fluorescence decay function F(t) of the probe molecule as

$$I_{||} = {}^1/_3F(t)(1 + 2r(t))$$

$$I_{\perp} = {}^1/_3F(t)(1 - r(t)) \quad (1)$$

The anisotropy decay is governed by the dynamical behavior of the transition dipoles of the probe molecules in the vesicle membrane. If we make the usual assumption (Best et al., 1987; van Langen et al., 1987; van Gurp et al., 1989; Muller et al., 1994a,b) that the DPH moiety in TMA-DPH and DPHPC is an effectively cylindrically symmetric molecule with its absorption transition dipole moment lying along its long molecular symmetry axis, the anisotropy can be written as a sum of three correlation functions $G_k(t)$, $k = 0, 1, 2$:

$$r(t) = r(t = 0)(G_0(t) + 2G_1(t) + 2G_2(t)) \quad (2)$$

The fundamental anisotropy $r(t = 0)$ is independent of the motion of the probe and is determined by the relative orientation of the absorption and emission transition dipole moments; in view of our assumption above, it is given by $r(t = 0) = 0.4P_2(\cos(\beta_v))$, where P_2 is the second Legendre polynomial and β_v is the angle between the emission dipole and the long molecular symmetry axis of DPH. The correlation functions describe the average correlation which exists between the directions of the long molecular axis at the moments of excitation and emission.

Standard models—i.e., the Brownian rotational diffusion (BRD) (Nordio & Segre, 1971; Zannoni et al., 1983; Arcioni et al., 1991) and the wobble-in-cone (WIC) model (Kinosita et al., 1977, 1984; Lipari & Szabo, 1981)—have a number of undesirable features. Analysis with those models predicts a substantial probability of finding populations of probe molecules parallel to the bilayer surface. This is reflected in the bimodal character of the orientational distribution function. This feature seems hard to reconcile with the polar nature of the TMA-DPH headgroup. These conceptual problems are avoided in the compound motion model (CMM; van der Sijs et al., 1993; van der Heide et al., 1993; Muller et al., 1994a,b) where good fits to time-resolved fluorescence data can be obtained with unimodal orientational distribution functions of the fluorescent probes. In particular, the CMM does not require the presence of a parallel population to explain the data. This model assumes that the probe molecules experience rapid, though restricted movements within a fluctuating free volume in the lipid bilayer, which is modeled as a slowly rotating cage or cone. To compute the anisotropy decay, we need the correlation functions $G_k(t)$, $k = 0, 1, 2$. These can be found by establishing the relation between the orientations of the local bilayer normal and the emission dipole of the fluorescing probe molecule. To simplify matters, we take that the fast motion within the cone is independent of the much slower motion of the cone itself. This implies that the correlation functions can be expressed as simple products of the correlation functions of both contributing single potentials:

$$G_k(t) \equiv G^{\mathrm{BF}}{}_k(t) = \sum_{m=-2}^{2} G^{\mathrm{BC}}{}_{km}(t)G^{\mathrm{CF}}{}_{m0}(t), \quad k = 0, 1, 2 \quad (3)$$

Here BF, BC, and CF refer to the orientational transformations from bilayer to fluorophore molecule, from bilayer to cone and from cone to fluorophore molecule frames of reference, respectively.

Furthermore, in the following we assume that the dynamics of the slowly rotating cone can be adequately described by the Brownian rotational diffusion (BRD) model, while the fast motion can be represented by strong collision dynamics with one jump time τ_{SC} within a rigid cone; the latter motion was therefore dubbed strong collision in cone (SCIC) (Muller et al., 1994a). Thus the present model is a compound of the BRD and the SCIC model. For the slow cone motion itself a potential U_{BC} still has to be specified. The choice for the BRD approach entails that the cone containing the probe molecules undergoes small step diffusion in an angle-dependent ordering quasipotential $U(\beta)$ mimicking the influence of the lipid environment. In view of their physicochemical properties the probes TMA-DPH and DPHPC, with their polar headgroup anchored at the bilayer–water interface, have very low probability of undergoing a flip-flop movement in the lipid bilayer. Furthermore, the apolarity of the DPH moiety rules out the possibility that it resides in the water phase at the bilayer–water interface. This implies that the probability must be negligible of finding the DPH moiety of both probes at angles larger than 90° with the local bilayer normal. This requirement led us to the choice of the following λ_1–λ_4 potential for the slow cone motion:

$$U(\beta_{\mathrm{BC}}) = -\lambda_1 P_1(\cos(\beta_{\mathrm{BC}})) - \lambda_4 P_4(\cos(\beta_{\mathrm{BC}})) \quad (4)$$

as was discussed previously (Muller et al., 1994a). Using this potential, the microscopic orientational distribution function $f(\beta_{\mathrm{BC}})$ for the cone director can be defined; this function describes the probability of finding the DPH moiety at an angle β_{BC} between the cone director and the bilayer normal:

$$f(\beta_{\mathrm{BC}}) = N \exp(-U(\beta_{\mathrm{BC}})) \quad (5)$$

where the factor N normalizes the distribution. The relevant first four order parameters for the cone director are then given by the following averages over the Legendre polynomials P_L:

$$\langle P_L \rangle_{\mathrm{BC}} = \int d\beta_{\mathrm{BC}} \sin(\beta_{\mathrm{BC}}) f(\beta_{\mathrm{BC}}) P_L(\cos(\beta_{\mathrm{BC}})), \quad L = 1, \ldots, 4 \quad (6)$$

For analytical expressions corresponding to the exceptionally simple λ_1 BRD potential the reader is referred to the appendix of Muller et al. (1994a). Those formulae also give a good approximation for the order parameters of a λ_1–λ_4 potential, provided λ_4 is relatively small.

The compound motion model contains two independent dynamical parameters, i.e., $D_\perp$ and $d_\perp$, which parameterize the slow tumbling of the cone around the probe and the much faster strong collision-in-cone motion of the probe itself respectively. The fast perpendicular diffusion coefficient $d_\perp$ is accordingly defined as the inverse of the strong collision jump time: $d_\perp = 1/\tau_{SC}$. We note that in the limit of a zero

cone-angle θ_{cone} the compound motion model reverts to a simple single BRD model without internal motion, so that then $G^{CM}{}_{m0}(t) = \delta_{m0}$ in eq 3. The anisotropy experimental data are insensitive to the value of $D_{||}$, which describes the rotational motion of the cone around its director, as long as the cone stays relatively narrow. Therefore we arbitrarily fix this parameter to $D_{||} = 5D_{\perp}$.

The λ_1 and λ_4 parameters for the membrane BRD potential and the cone angle θ_{cone} account for the order of the probe in the membrane. The order parameters $\langle P_L \rangle_{BF}$ characterize the order of the long axis of the fluorophore with respect to the local bilayer normal. Due to the extra degree of freedom of motion in the cone, these appear as products of order parameters $\langle P_L \rangle_{BC}$ of the cone director (cf. eq 6) and order parameters $\langle P_L \rangle_{CF}$ of the long molecular axis with respect to the cone:

$$\langle P_L \rangle_{BF} = \langle P_L \rangle_{BC} \langle P_L \rangle_{CF} \tag{7}$$

with $L = 1, 2, \ldots$. The $\langle P_L \rangle_{CF}$ are calculated using the standard expressions for wobble-in-cone model as given in the appendix of Muller et al. (1994a).

Numerical Methods. The numerical analysis of the time-resolved experimental data was carried out using the ZXSSQ FORTRAN routine from the IMSL programme library to fit the data to the model with the nonlinear least-squares method of Levenberg and Marquardt. The experimental decay curves from the time-resolved experiment were analyzed using a reiterative nonlinear least-squares deconvolution technique (Cundall & Dale, 1983). By integrating the decays in parallel and perpendicular polarization values for the steady-state anisotropy r_{ss} were calculated. These were independently confirmed for a number of systems by steady-state measurements using a SPF 500 SLM-Aminco spectrofluorimeter equipped with polarizers. Analysis of the anisotropy decay curves yielded the fluorescence decay as a byproduct. As a cross-check the values of these decay parameters have been compared for a number of samples with those obtained directly from an independent fluorescence intensity decay measurement. The fluorescence decay could be well fitted to a biexponential decay function with preamplitudes α_1 and α_2 and lifetimes τ_1 and τ_2. In all cases tested, excellent agreement between the outcomes of both methods was found for both TMA-DPH and DPHPC. The mean fluorescence lifetime is defined by the normalized first moment of the decay function as

$$\langle \tau_F \rangle = \sum_{i=1,2} \alpha_i \tau_i^2 / \sum_{i=1,2} \alpha_i \tau_i \tag{8}$$

In the anisotropy model fit the following 11 free parameters were optimized: (1−2) the fluorescence decay amplitudes α_1 and α_2, (3−4) the fluorescence decay exponents τ_1 and τ_2, (5) the factor $P_{2\beta\nu} = P_2(\cos(\beta_\nu))$, where β_ν is the emission dipole angle in the molecular frame, (6−7) the BRD potential parameters λ_1 and λ_4, (8) the slow rotational diffusion coefficient $D_\perp$ for the motion of the cone containing the probe, (9) the SCIC cone angle θ_{cone}, (10) the SCIC fast diffusion coefficient $d_\perp$ of the probe within the cone, and (11) a parameter to account for a time shift between the excitation profile and both fluorescence emission signals.

RESULTS AND DISCUSSION

We have investigated the effect of the small peptide gA on the molecular orientational order and dynamics of TMA-DPH and DPHPC in various unilamellar lipid vesicles. To this end, time-resolved fluorescence anisotropy and lifetime measurements were performed. The analysis of the anisotropy data was done with the compound motion model (CMM).

Table 1: Effect of Gramicidin A on the Steady-State Fluorescence Anisotropy and Lifetimes for the Probes TMA-DPH and DPHPC Embedded in Unilamellar Lipid Vesicles of DMPC in the Liquid Crystalline Lipid Phase at 35 °C[a]

molar ratio gramicidin A	R_{ss}	α_1	τ_1 (ns)	α_2	τ_2 (ns)	$\langle \tau_F \rangle$ (ns)
probe: TMA-DPH						
0%	0.180	0.21	1.5	0.79	4.6	4.4
2%	0.195	0.36	1.4	0.64	5.2	4.7
probe: DPHPC						
0%	0.155	0.17	4.9	0.83	7.5	7.2
2%	0.177	0.13	4.0	0.87	7.7	7.4
5%	0.187	0.15	3.9	0.85	7.9	7.6

[a] The peptide to lipid molar ratio is specified in percentages. gA was incorporated from ethanolic solution. The estimated uncertainties are R_{ss}, 0.003; lifetime parameters α_1, τ_1, α_2, τ_2, and $\langle \tau_F \rangle$, 5%.

DMPC Vesicles. To start with, we incorporated gA in DMPC vesicles. This short-chain lipid ($n_{carbon} = 14$) has been used frequently to study the effect of gA [see, e.g., the review by Killian (1992) and Morrow et al. (1991) and Bouchard and Auger (1993)]. The transition temperature for pure DMPC is $T_{tr} = 23$ °C (Chapman et al., 1977); however, it has been reported that the presence of gA considerably broadens the phase transition region of DMPC (Morrow et al., 1991). We therefore performed our experiments on DMPC vesicles at 35 °C. Table 1 gives steady-state fluorescence anisotropy and lifetime results for DMPC vesicles with 0, 2, or 5 mol % gA added from ethanolic solution. As a consequence of its solvent history, gA was embedded in the lipid matrix in the nonchannel conformation.

The results from steady-state anisotropy measurements are listed in Table 1. It can be seen that gA induces a rise in r_{ss} and the mean lifetime $\langle \tau_F \rangle$ as well. There are several possible explanations for this increase in the steady-state anisotropy r_{ss}. It may be induced by (a) higher order as expressed by the $\langle P_L \rangle$, $L = 1, \ldots, 4$, (b) slower rotational diffusion $D_\perp$, or (c) reduction of fluorescence lifetimes τ_i, $i = 1, 2$, or an arbitrary combination of these. The separate contributions can only be disentangled by time-resolved anisotropy experiments.

This is undertaken in Table 2, where corresponding parameters are given, which were extracted from the time-resolved data using the CMM. This model allowed good fits to the data, as indicated by the values for χ^2_{red} in the second column of Table 2. In the third column values for the emission dipole moment angle β_ν are shown which are in line with previous findings for both probes (van Langen et al., 1987, 1989; Ameloot et al., 1984; Muller et al., 1994a,b). In the fourth and fifth columns the λ parameters of the BRD potential for the slow motion of the cone are given. The auxiliary λ_4 parameter values are much smaller than those for λ_1 as is required both for a unimodal orientational probe distribution and for the stability of the fitting algorithm as discussed previously (Muller et al., 1994a). The rotational diffusion parameter $D_\perp$ in the sixth column is seen to decrease 20−50% with increasing gA concentration. The width of the cone for fast motion reflects the restriction of the probe motion due to the fluctuating free volume in between lipid acyl chains. As shown in column

Table 2: Effect of Gramicidin A on the Time-Resolved Fluorescence Anisotropy of TMA-DPH and DPHPC Embedded in Unilamellar Lipid Vesicles of DMPC in the Liquid Crystalline Phase at 35 °C Interpreted in Terms of the Compound Motion Model[a]

molar ratio gramicidin A	χ^2_{red}	β_ν (deg)	λ_1	λ_4	$D_\perp$ (ns)	θ_{cone} (deg)	$d_\perp$ (ns)	$\langle P_1\rangle$	$\langle P_2\rangle$	$\langle P_3\rangle$	$\langle P_4\rangle$
probe: TMA-DPH											
0%	1.31	13	6.2	0.5	0.042	27	2	0.82	0.55	0.32	0.16
2%	1.48	15	5.7	0.8	0.034	23	2	0.83	0.58	0.36	0.20
probe: DPHPC											
0%	1.38	21	5.8	0.2	0.027	24	3	0.80	0.52	0.28	0.13
2%	1.29	21	8.0	0.3	0.017	26	1	0.84	0.60	0.36	0.19
5%	1.20	22	7.4	0.9	0.013	24	1	0.86	0.65	0.43	0.25

[a] The gA to lipid ratio is indicated as a percentage. The peptide was incorporated from ethanolic solution. The overall order parameters $\langle P_L\rangle_{FB}$, $L = 1, ..., 4$ for the fluorophore with respect to the bilayer are calculated using λ_1, λ_4, and θ_{cone}. The estimated uncertainties are β_ν, 2°; λ_1, 5%; λ_4, 0.3; $D_\perp$, 20%; θ_{cone}, 3°; $d_\perp$, 40%; and overall order $\langle P_L\rangle$ parameters, 3%.

seven, effects on this width depend on the probe used. For TMA-DPH, the cone is narrowed by gA, while it remains unaffected for DPHPC. This is a first indication that the magnitude of the structural perturbation by gA varies with the depth in the bilayer. This point will be discussed more thoroughly below.

In accordance with the assumptions of CMM, the fast diffusion coefficient $d_\perp$ for the rattling motion of the probe in the cone given in column eight is typically two orders of magnitude larger than the diffusion coefficient $D_\perp$ of the cone itself. The effects of gA on membrane structure are reflected by the order parameters $\langle P_L\rangle_{FB}$, $L = 1, ..., 4$ in the last four columns. It is clear that gA enhances the overall order of both TMA-DPH and DPHPC, as exemplified by the rise in $\langle P_2\rangle_{FB}$ for both probes in the tenth column; however, the order of DPHPC is seen to rise more steeply than that of TMA-DPH. This suggests that the ordering effect of gA is stronger in the hydrocarbon region of the DMPC bilayer probed by DPHPC than in the upper part of the acyl-chain region monitored by TMA-DPH. These findings corroborate previous deuterium NMR studies (Rice & Oldfield, 1979); they have shown that gramicidin at moderate concentrations (up to about 10 mol %) increases the quadrupole splitting, which is a measure for order, of selectively deuterated DMPC hydrocarbon chains at positions 2−14. In addition, our time-resolved studies revealed effects of gA on the dynamics of the lipid molecules.

POPC, EGGPC, DLPC, and SQDG Vesicles. Further experiments were done on gA doped vesicles of POPC, EGGPC, and DLPC. These phospholipids differ from DMPC by their longer acyl chains ($n_{carbon} \geq 16$) and increasing unsaturation. Moreover, DOPG and the plant lipid SQDG were investigated, which are characterized by a radically different headgroup. In all cases, gA was added from an ethanolic solution and was thus incorporated in the lipid bilayer in the nonchannel conformation. The results for the steady-state anisotropy and lifetime for TMA-DPH are given in Table 3. Addition of gA causes in a molar concentration of 1:50 causes the steady-state anisotropy to rise systematically about 10% for all the lipids studied. The mean fluorescence lifetimes $\langle\tau_F\rangle$ for TMA-DPH are likewise enhanced typically 20% in the presence of gA, except for DLPC where $\langle\tau_F\rangle$ is hardly affected.

Table 4 summarizes the results from the time-resolved anisotropy decays of TMA-DPH. As with DMPC, the CMM gives good fits to the data. The values for the emission dipole angle β_ν are seen to be in the range of 16 ± 3°; such numbers are independently confirmed by steady-state fluorescence experiments on the TMA-DPH immobilized in a PVA polymer film (data not shown).

Table 3: Effect of Gramicidin A on the Steady-State Fluorescence Anisotropy and Lifetimes of TMA-DPH Embedded in Unilamellar Lipid Vesicles[a]

molar ratio gramicidin A	R_{ss}	α_1	τ_1 (ns)	α_2	τ_2 (ns)	$\langle\tau_F\rangle$ (ns)
POPC						
0%	0.182	0.35	1.4	0.65	4.4	3.9
2%	0.206	0.40	1.2	0.60	5.0	4.5
EGGPC						
0%	0.187	0.37	1.2	0.63	4.1	3.7
2%	0.206	0.46	1.2	0.54	4.8	4.1
DLPC						
0%	0.167	0.44	0.9	0.56	3.0	2.6
2%	0.184	0.45	1.0	0.55	3.3	2.8
DOPG						
0%	0.216	0.37	1.1	0.63	3.5	3.1
2%	0.233	0.52	1.5	0.48	4.3	3.6
SQDG						
0%	0.215	0.38	1.1	0.62	3.0	2.7
2%	0.237	0.38	1.6	0.62	4.8	4.2

[a] For each sample the concentration of gA, which was added from ethanol solution, is indicated in molar percentages. The estimated uncertainties are R_{ss}, 0.003; lifetime parameters α_1, τ_1, α_2, τ_2, and $\langle\tau_F\rangle$, 5%. The temperature was 20 °C.

Generally, addition of gA is seen to reduce the diffusion coefficient $D_\perp$ for the cone in the bilayer. As the error in the diffusion parameters is estimated at around 20%, these changes are significant. They suggest a slowing down of the reorientation of the cone containing the probe in the bilayer. This decrease in lipid dynamics can be related to NMR work on labeled gramicidin (Koeppe et al., 1994) and high pressure intrinsic fluorescence studies (Scarlata, 1991); these studies point out the role played by hydrogen bonds between the gramicidin indole hydrogens and the carbonyl groups of the surrounding lipids which could account for the reduced dynamics. However, our findings for DLPC where gA does not reduce $D_\perp$, seem to contradict this explanation.

The fast diffusion coefficient $d_\perp$ for the probe motion within the assumed cone is seen to be reduced by gA. As discussed previously (Muller et al., 1994a), these values represent only lower bounds, because the time resolution used in the present experiments does not allow an accurate determination of these very fast motions. The orientational order parameters $\langle P_L\rangle_{BF}$, $L = 1, ..., 4$ for the probe with respect to the bilayer normal are typically 10% higher in the presence of 2 mol % of gA, except in the case of DOPG, where a small but significant disordering is suggested by the data. This could be a headgroup effect. It is seen that for DOPG the effect of the reduced dynamics on r_{ss} more than counterbalances the effect of the reduced order, so that

Table 4: Effect of Gramicidin A on the Time-Resolved Fluorescence Anisotropy of TMA-DPH Embedded in Unilamellar Lipid Vesicles Interpreted in Terms of the Compound Motion Model[a]

molar ratio gramicidin A	χ^2_{red}	β_ν (deg)	λ_1	λ_4	$D_\perp$ (ns)	θ_{cone} (deg)	$d_\perp$ (ns)	$\langle P_1 \rangle$	$\langle P_2 \rangle$	$\langle P_3 \rangle$	$\langle P_4 \rangle$
POPC											
0%	1.31	15	5.8	0.0	0.045	22	5	0.80	0.51	0.26	0.11
2%	1.96	18	6.9	0.0	0.027	19	3	0.83	0.57	0.33	0.16
EGGPC											
0%	1.31	16	5.9	0.0	0.040	23	3	0.80	0.51	0.27	0.12
2%	1.78	19	6.1	0.0	0.020	22	2	0.81	0.53	0.28	0.13
DLPC											
0%	1.64	15	4.2	0.2	0.044	30	4	0.72	0.38	0.16	0.05
2%	1.78	19	3.7	0.6	0.045	22	2	0.74	0.44	0.24	0.13
DOPG											
0%	1.16	13	3.8	0.7	0.034	21	2	0.74	0.45	0.25	0.14
2%	1.73	15	4.0	0.2	0.020	19	2	0.74	0.42	0.20	0.09
SQDG											
0%	1.30	13	4.6	0.9	0.040	23	2	0.80	0.54	0.33	0.19
2%	1.25	13	6.2	0.5	0.019	21	2	0.84	0.60	0.38	0.21

[a] Gramicidin A was added to the lipids from an ethanol solution prior to the vesicle preparation; the peptide to lipid ratio is indicated as a percentage. The overall order parameters $\langle P_L \rangle_{FB}$, $L = 1, ..., 4$ for the fluorophore with respect to the bilayer are calculated using λ_1, λ_4, and θ_{cone}. From the variation in the values of chisquare reduced, the uncertainties in the fitting parameters are estimated as β_ν, 2°; λ_1, 5%; λ_4, 0.3; $D_\perp$, 20%; θ_{cone}, 3°; $d_\perp$, 40%; and overall order $\langle P_L \rangle$ parameters, 3%. The temperature was 20 °C.

r_{ss} is increased by gA. We note that for vesicle systems of the plant lipid SQDG the behavior is in line with the general picture of reduced dynamics and slightly increased order.

The different headgroups of the PC lipids POPC and EGGPC on the one hand and the polar sulfolipid SQDG on the other are seen to be irrelevant for this general action of gramicidin as sensed by TMA-DPH. However, we cannot rule out a possible electrostatic interaction between the positive charged TMA group and the negative lipid headgroup of SQDG and also DOPG. Surprisingly, DOPG/gA vesicles were found here to be an exception to the rule that gA orders the probes as it causes a small but significant lowering of the $\langle P_L \rangle$, $L = 1, ..., 4$ in Table 4. It was found earlier by Killian et al. (1986) that gA can strongly affect the macroscopic structure of DOPG in emulsion. In a ^{31}P and X-ray diffraction study they showed that gA can induce an inverted hexagonal H_{II} lipid phase in a DOPG emulsion.

For POPC/gA vesicles Cox et al. (1992) found significant conformational effects on the steady state anisotropy of DPH, comparable with the one to be discussed below for DOPC/gA systems studied with DPHPC. It is therefore reasonable to assume that additional studies of POPC/gA vesicles with the DPHPC probe at greater depths in the hydrophobic bilayer core would also detect different effects of the channel and nonchannel conformations of gA.

DOPC Vesicles. Finally, we discuss our results for DOPC/gA unilamellar vesicles, which were studied with both the TMA-DPH and DPHPC probes. These systems were investigated in greater detail as gA modulates the phase of emulsions of the same lipid in a concentration dependent way; then gA can induce an inverted hexagonal H_{II} phase (Killian et al 1987). However, it is only in the channel conformation that gA performs this trick (Tournois et al., 1987, 1988). To study the effect of the channel and nonchannel conformations, we incorporated gA in DOPC unilamellar vesicles from both trifluoroethanol and ethanol solutions. Peptide to lipid molar ratios ranging from 1:100 to 1:10, i.e., 1 up to 10 molar % were used.

Figure 2 displays the steady-state fluorescence anisotropies r_{ss} for TMA-DPH and DPHPC in DOPC vesicles containing 0, 1, 2, and 10 molar % of gA. In all cases the r_{ss} values for TMA-DPH are much higher than those for DPHPC; this

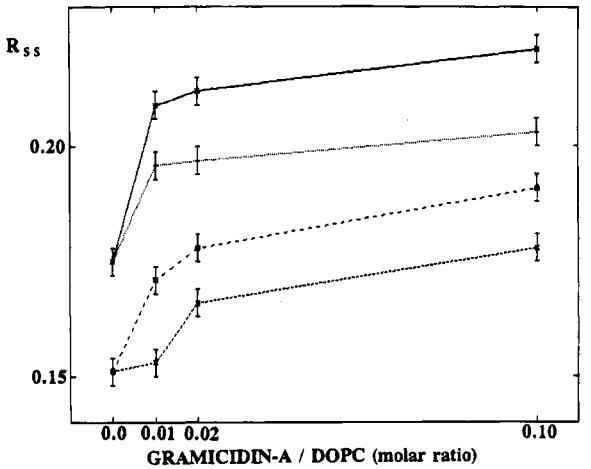

FIGURE 2: Steady-state fluorescence anisotropy r_{ss} of TMA-DPH and DPHPC in DOPC vesicle bilayers containing various amounts of gramicidin A cosolubilized either from ethanol or trifluoroethanol. Results are specified as follows. (Upper pair of curves) TMA-DPH, channel conformation (★); TMA-DPH, nonchannel conformation (+). (Lower pair of curves) DPHPC, nonchannel conformation (□); and DPHPC, channel conformation (×). The solvent-induced conformations of gA are shown to differ in their effect at the depths in the lipid bilayer probed by TMA-DPH and DPHPC.

can be rationalized in terms of the different locations of the fluorophore DPH in both probes within the lipid bilayer (e.g., Cranney et al., 1983; van Langen et al., 1989; Ferretti et al., 1993). In Figure 2 a striking difference between the effects of gA on TMA-DPH and DPHPC comes to light: while the r_{ss} rises for both probes with increasing concentration of gA, the effect of the two conformations on the probes is opposite. The nonchannel conformation induces a higher r_{ss} for DPHPC than the channel conformation, in contrast to the effect on TMA-DPH where the situation is reversed. The average lifetime $\langle \tau_F \rangle$ of TMA-DPH shown in Table 5 is enhanced in the presence of gA, independent of its concentration in the vesicle. In contrast, the average lifetime of DPHPC is not increased significantly by gA in either conformation. This suggests that near the bilayer surface effects of gA occur that can be sensed by TMA-DPH but not by DPHPC deeper in the bilayer. These trends in both the steady-state anisotropy and the fluorescence lifetime are

Table 5: Effect of the Conformation of Gramicidin A on the Fluorescence Lifetime Parameters of TMA-DPH and DPHPC Embedded in Unilamellar Lipid Vesicles of DOPC[a]

molar ratio gramicidin A	α_1	τ_1 (ns)	α_2	τ_2 (ns)	$\langle\tau_F\rangle$ (ns)
probe: TMA-DPH					
0%	0.45	1.2	0.55	3.8	3.2
1% nonch	0.47	1.2	0.53	4.3	3.7
1% ch	0.50	1.2	0.50	4.5	3.8
2% nonch	0.53	1.4	0.47	4.5	3.7
2% ch	0.49	1.3	0.51	4.4	3.7
10% nonch	0.50	1.2	0.50	4.5	3.8
probe: DPHPC					
0%	0.28	1.6	0.72	7.1	6.7
1% nonch	0.29	3.4	0.71	7.5	6.8
1% ch	0.30	3.7	0.70	7.6	6.9
2% nonch	0.30	3.4	0.70	7.5	6.8
2% ch	0.35	4.0	0.65	7.7	6.9
10% nonch	0.34	3.1	0.66	7.6	6.9
10% ch	0.28	2.6	0.72	7.4	6.8

[a] The molar gramicidin to lipid ratio is given for each sample. By codissolving gA from TFE (ETOH), its induced conformation was the channel (nonchannel) one; for each sample this conformation is indicated. The estimated uncertainties are 5% for α_1, τ_1, α_2, τ_2, and $\langle\tau_F\rangle$. The temperature was 20 °C.

indications that the effects of gA depend on the depth in the bilayer.

The results for time-resolved anisotropy summarized in Table 6 enable us to disentangle the effects of the order and dynamics on the steady-state and time-resolved anisotropy. Again, the application of the CMM allowed good fits to the data and yielded reasonable parameter values for λ_1, λ_4, $D_\perp$, θ_{cone}, and $d_\perp$ in accordance with the assumptions of the model as discussed previously. Figure 3 shows a typical fit to the data for DOPC/gA/DPHPC vesicles at the peptide to lipid molar ratio 1:100 where gA was added from ethanolic solution. Table 6 shows that, as found above for other systems, the slow rotational diffusion coefficient $D_\perp$ for the cone is reduced by gA for both TMA-DPH and DPHPC, irrespective of the conformation. For two samples indicated with asterisks, the time-resolution of 80 ps/channel of DPHPC measurements is so coarse that the emission dipole angle β_ν and the cone half-angle θ_{cone} remain highly correlated as both determine the drop in anisotropy on short time scales (Muller et al., 1994a); for those samples their contributions cannot be disentangled. However, as the fast motion within the cone is independent from the slow motion of the cone itself, the slow parameters remain well determined.

The last four columns of Table 6 display the order parameters. These reflect the effect of gA on the orientational distribution of the fluorescent probes. At first sight, we find that gA always increases molecular order, irrespective of the gA conformation or probe used. Upon closer inspection, two interesting observations can be made. First, the gA induced increase in molecular order is higher for DPHPC than for TMA-DPH. This strongly suggests that the effect of gA varies with the depth in the hydrocarbon region of the lipid bilayer. Second, for the DPHPC probe the nonchannel conformation of gA is more effective than the channel conformation in increasing molecular order. For TMA-DPH the role of conformation is reversed, i.e., the channel conformation is more effective. This suggests that the ordering effect of the nonchannel conformation is more prominent at greater depth in the bilayer. If so, this finding correlates well with results from Cox et al. (1992). These authors considered effects from channel and nonchannel gA embedded in POPC vesicles doped with the fluorescent probe DPH. In view of its apolar nature, this probe is located at the center of the bilayer. From steady-state anisotropy experiments Cox et al. reported the nonchannel conformation of gA to be more effective for increase in molecular order of the DPH probes. Conformational effects of gA on the surrounding lipid molecules in the lamellar phase are also found by others for DMPC with different techniques (Morrow et al., 1991; Bouchard & Auger, 1993). Their results showed that in the liquid crystalline phase of DMPC films the conformation of gA affects the orientational order and the orientation of the tryptophan side chains and their interaction with the hydrocarbon chains. Returning to the case of DPHPC, the implications of the gA for the shape of the orientational distribution function are illustrated in Figure 4, where the ordering effect of nonchannel gA is clearly visible.

The conformation and probe dependent ordering effects of gA on DOPC vesicles reported above are likely to be related to the strain that is exerted by gA on the supporting lipid matrix. The probe-dependent effect can be rationalized as follows. TMA-DPH and DPHPC differ from each other in various respects, e.g., their geometry and inertial mass which must have consequences for their behavior in the bilayer. Nevertheless, we believe it is here the location of their DPH-fluorophore that is the most consequential for their differing response to the presence of gA (Muller et al., 1994b). This means that the effect of gA depends on the depth in the bilayer. By implication, the values for $\langle P_2\rangle_{FB}$ of both probes are a crude measure for the change in the order profile along the lipid chains caused by gA.

We tentatively propose that the conformational effect on the $\langle P_2\rangle$ order parameter in DOPC unilamellar vesicles is a reflection of the difference in geometrical form of the channel and nonchannel conformations of gA. Current models picture the gA dimer in the channel conformation as diabolo-shaped, with the bulky tryptophan residues near the C-terminal at the bilayer−water interface and a waist where the N-terminals of both gA molecules join. In contrast, the nonchannel conformation, e.g., the double-stranded antiparallel helical dimer, has a roughly cylindrical shape (Killian, 1992). This entails that gA channels constrain the upper acyl chain regions of adjacent lipid molecules to a larger extent than the lower regions due to the conical geometry of each of the gA monomers in this conformation. This could give rise to a different order parameter profile than that induced by the nonchannel gA conformation, as the latter has a more cylindrical shape. This conformational effect on the order parameter profile in DOPC could be validated by using other techniques. In particular we think of deuterium NMR of labeled lipids or using anthroyl fatty acid as depth-selective fluorescent probes. On the basis of the results presented here, we predict a significant dependence on the depth in the bilayer.

Summarizing, we have shown that time-resolved fluorescence lifetime and anisotropy measurements on probes can be used fruitfully to study the effects of gramicidin on lipid vesicle membranes. Time-resolved experiments were required to obtain separate information on the structural and dynamical parameters of the probes in the vesicle bilayer. In particular, the novel compound model turned out to be a

Table 6: Effect of the Conformation of Gramicidin A on the Time-Resolved Fluorescence Anisotropy of TMA-DPH and DPHPC Embedded in Unilamellar Lipid Vesicles of DOPC Interpreted in Terms of the Compound Motion Model[a]

molar ratio gramicidin A	χ^2_{red}	β_ν (deg)	λ_1	λ_4	$D_\perp$ (ns)	θ_{cone} (deg)	$d_\perp$ (ns)	$\langle P_1 \rangle$	$\langle P_2 \rangle$	$\langle P_3 \rangle$	$\langle P_4 \rangle$
probe: TMA-DPH											
0%	1.42	17	4.5	0.2	0.034	29	2	0.74	0.41	0.18	0.07
1% nonch	1.70	18	5.2	0.1	0.028	24	1	0.77	0.46	0.22	0.08
1% ch	1.56	15	5.2	0.1	0.025	23	1	0.78	0.48	0.24	0.10
2% nonch	1.56	20	5.1	−0.1	0.021	24	2	0.76	0.45	0.21	0.07
2% ch	1.71	16	4.6	0.6	0.029	21	2	0.79	0.52	0.30	0.17
10% nonch	1.69	16	5.4	−0.2	0.030	21	2	0.78	0.48	0.23	0.08
probe: DPHPC											
0%	1.98	12	2.2	0.2	0.023	28	2	0.54	0.20	0.06	0.02
1% nonch	1.26	19	3.5	0.5	0.017	25	2	0.71	0.38	0.18	0.09
1% ch	1.62	*	3.9	0.1	0.015	*	*	0.70	0.35	0.13	0.03
2% nonch	1.60	19	4.3	0.3	0.016	25	2	0.75	0.44	0.21	0.09
2% ch	1.52	*	4.5	0.0	0.013	*	*	0.74	0.42	0.19	0.06
10% nonch	1.40	21	5.3	0.0	0.013	21	1	0.78	0.49	0.25	0.10

[a] The overall order parameters $\langle P_L \rangle_{FB}$, $L = 1, ..., 4$ for the fluorophore with respect to the bilayer are calculated using λ_1, λ_4, and θ_{cone}. The estimated uncertainties are β_ν, 3°; λ_1, 5%; λ_4, 0.3; $D_\perp$, 20%; θ_{cone}, 3°; $d_\perp$, 40%; and overall order $\langle P_L \rangle$ parameters, 3%. The molar gA to lipid ratio and gA conformation is indicated for each sample. An asterisk denotes a unresolved parameter due to low time-resolution as discussed in the main text. The temperature was 20 °C.

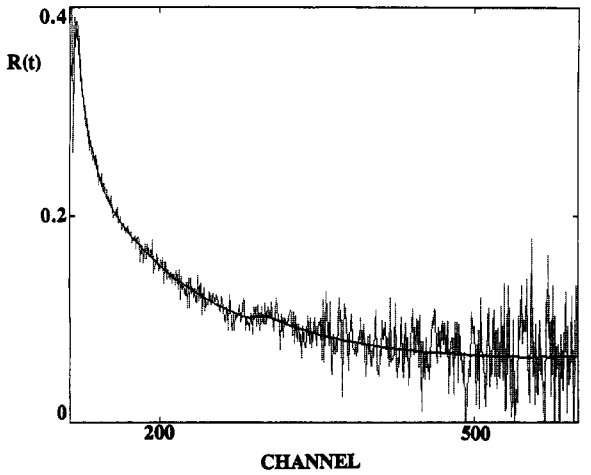

FIGURE 3: Time-resolved fluorescence anisotropy of DPHPC in DOPC/gA/DPHPC 1:100 unilamellar vesicles. gA was cosolubilized from ethanolic solution and is therefore in the nonchannel conformation. Data (dashed line) and corresponding fit (drawn line) using the compound motion model are shown.

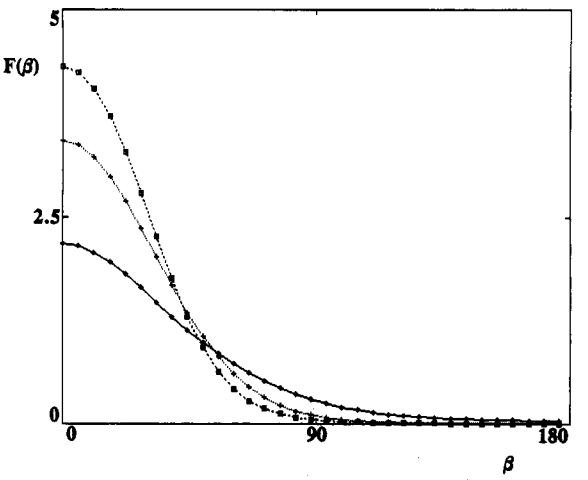

FIGURE 4: Ordering effect of gramicidin A. Orientational distribution functions $f(\beta)$ for DPHPC embedded in unilamellar vesicle systems DOPC in a gA/lipid molar ratio of 0 (◇), 1 (+), and 10 (□) molar %. The peptide gA was added from ethanolic solution before the vesicle preparation. The distribution is reconstructed using the global order parameters $\langle P \rangle_{FB}$ given in Table 6. β is the angle of the long molecular axis of the probe with respect to the local lipid bilayer normal.

useful model in the data analysis. This is the first application of this model to study peptide−lipid interactions. It was found that the effect of nonchannel gA in unilamellar lipid model vesicles depends on its concentration and the depth at which the hydrophobic region of the lipid bilayer is probed. In general, gA increases the orientational order while decreasing the reorientational dynamics in the concentration regimes studied here. In the case of DOPC, both channel and nonchannel conformations of the peptide were compared. In unilamellar vesicles of this lipid, the two conformations of gA could be clearly distinguished by their effect on the order parameter profile. Channel (nonchannel) gA is more effective in the upper (deeper) acyl region of the bilayer. This can be rationalized in terms of the different shapes of the gA dimer in its channel and nonchannel conformations.

ACKNOWLEDGMENT

We gratefully acknowledge Drs. J. A. Killian, H. Tournois, and T. C. B. Vogt [Center for Biomembranes and Lipid Enzymology (CBLE), University of Utrecht] for fruitful discussions, the generous gift of the vital HPLC purified gramicidin A, and access to CD instrumentation, and Mrs. M. de Jong-Verheijden for running numerous fluorescence spectra. The SRS (Synchrotron Radiation Source, Daresbury, U.K.) was made available by an agreement between SERC (Scientific and Engineering Research Council) and NWO (Netherlands Organization for Scientific Research). We thank Drs. D. Shaw, M. Martin and M. Behan-Martin, for practical help and discussions at Daresbury Laboratory (U.K.).

REFERENCES

Ameloot, M., Hendrickx, H., Herreman, W., Pottel, H., van Cauwelaert, F., & van der Meer, W. (1984) *Biophys. J. 46*, 525−539.

Andersen, O. S. (1984) *Annu. Rev. Physiol. 46*, 531−548.

Andersen, O. S., Sawyer, D. B., & Koeppe, R. E., II (1992) in *Biomembrane Structure and Function* (Gaber, B. P., & Easwaran, K. R. K., Eds.) pp 227−244, Adenine Press, Schenectady, NY.

Arcioni, A., Tarroni, R., & Zannoni, C. (1991) *J. Chem. Soc., Faraday Trans. 87*, 2457−2466.

Bañó, M. C., Braco, L., & Abad, C. (1989) *FEBS Lett. 250*, 67−71.

Bañó, M. C., Braco, L., & Abad, C. (1991) *Biochemistry 30*, 886–894.
Best, L., John, E., & Jaehnig, F. (1987) *Eur. Biophys. J. 15*, 87–102.
Bouchard, M., & Auger, M. (1993) *Biophys. J. 65*, 2484–2492.
Chapman, D., Cornell, B. A., Eliasz, A. W., & Perry, A. (1977) *J. Mol. Biol. 113*, 517–538.
Chen, P. S., Toribara, T. Y., & Warner, H. (1956) *Anal. Chem. 28*, 1756–1760.
Cornell, B. J. (1987) *J. Bioenerg. Biomembr. 19*, 655–676.
Cox, K. J., Ho, C., Lombardi, J. V., & Stubbs, C. D. (1992) *Biochemistry 31*, 1112–1118.
Cranney, M., Cundall, R. B., Jones, G. R., Richards, J. T., & Thomas, E. W. (1983) *Biochim. Biophys. Acta 735*, 418–425.
Cundall, R. B., & Dale, R. E., Eds. (1983) *Time-Resolved Fluorescence Spectroscopy in Biochemistry and Biology*, Plenum Press, New York.
Davies, M. A., Brauner, J. W., Schuster, H. F., & Mendelsohn, R. (1990) *Biochem. Biophys. Res. Commun. 168*, 85–90.
Ferretti, G., Tangorra, A., Zolese, G., & Curatola, G. (1993) *Membr. Biochem. 10*, 17–27.
Haigh, E. A., Thulborn, K. R., & Sawyer, W. H. (1979) *Biochemistry 18*, 3525–3532.
Ho, C., & Stubbs, C. D. (1992) *Biophys. J. 63*, 897–902.
Killian, J. A. (1992) *Biochim. Biophys. Acta 1113*, 391–425.
Killian, J. A., & de Kruijff, B. (1986) *Chem. Phys. Lipids 40*, 259–284.
Killian, J. A., & Urry, D. W. (1988) *Biochemistry 27*, 7295–7301.
Killian, J. A., van den Berg, C. W., Tournois, H., Keur, S., Slotboom, A. van Scharrenburg, G. J. M., & de Kruijff, B. (1986) *Biochim. Biophys. Acta 857*, 13–27.
Killian, J. A., Burger, K. N. J., & de Kruijff, B. (1987) *Biochim. Biophys. Acta 897*, 269–284.
Kinosita, K., Jr., Kawato, S., & Ikegami, A. (1977) *Biophys. J. 20*, 289–305.
Kinosita, K., Jr., Kawato, S., & Ikegami, A. (1984) *Adv. Biophys. 17*, 147–203.
Koeppe, R. E., Killian, J. A., & Greathouse, D. V. (1994) *Biophys. J. 66*, 14–24.
Lakowicz, J. R. (1986) *Principles of Fluorescence Spectroscopy*, Plenum Press, New York.
Lee, D. C., Durrani, A. A., & Chapman, D. (1984) *Biochim. Biophys. Acta 769*, 49–56.
Lipari, G., & Szabo, A. J. (1981) *Chem. Phys. 75*, 2971–2976.
Masotti, L., Cavatorta, P., Sartor, G., Casali, E., & Szabo, A. G. (1986) *Biochim. Biophys. Acta 862*, 265–272.
Mayer, L. D., Hope, M. J., & Cullis, P. R. (1986) *Biochim. Biophys. Acta 858*, 161–168.
Morrow, M. R., Simatos, G. A., Srinivasan, R., Grandal, N., Taylor, N., & Keough, D. M. W. (1991) *Biochim. Biophys. Acta 1070*, 209–214.
Muller, J. M., Moers, M. P. H., van de Poppe, D. J., van Ginkel, G., & Levine, Y. K. (1989) *Colloque INSERM 195*, 492.
Muller, J. M., van Faassen, E. E., & van Ginkel, G. (1994a) *Chem. Phys. 185*, 393–404.
Muller, J. M., van Faassen, E. E., & van Ginkel, G. (1994b) *Biochem. Biophys. Res. Commun. 201*, 709–715.
Nordio, P. L., & Segre, U. (1979) in *The molecular physics of liquid crystals* (Luckhurst, G. R., & Gray, G. W., Eds.) pp 411–426, Academic Press, New York.
Rice, D., & Oldfield, E. (1979) *Biochemistry 18*, 3272–3279.
Scarlata, S. F. (1988) *Biophys. J. 54*, 1149–1157.
Scarlata, S. F. (1991) *Biochemistry 30*, 9853–9859.
Spisni, A., Pasquali-Ronchetti, I., Casali, E., Lindner, L., Cavatorta, P., Masotti, L., & Urry, D. W. (1983) *Biochim. Biophys. Acta 732*, 58–68.
Tournois, H., Killian, J. A., Urry, D. W., Bokking, O. R., de Gier, J., & de Kruijff, B. (1987) *Biochim. Biophys. Acta 905*, 222–226.
Tournois, H., Henseleit, U., de Gier, J., de Kruijff, B., & Haest, C. W. M. (1988) *Biochim. Biophys. Acta 946*, 173–177.
Tournois, H., Fabrie, Ch. H. J. P., Burger, K. N. J., Mandersloot, J., Hilgers, P., van Dalen, H., de Gier, J., & de Kruijff, B. (1990) *Biochemistry 29*, 8297–8307.
Urry, D. W. (1985) in *The Enzymes of Biological Membranes* (Martonosi, A. N., Ed.) 2nd ed., Vol. 1, pp 229–257, Plenum Press, New York.
van der Heide, U. A., van Zandvoort, M. A. M. J., van Faassen, E. E., & Levine, Y. K. (1993) *J. Fluoresc. 3*, 269–277.
van der Sijs, D. A., van Faassen, E. E., & Levine, Y. K. (1993) *Chem. Phys. Lett. 216*, 559–565.
van Echteld, C. J. A., de Kruiff, B., Verkleij, A. J., Leunissen-Bijvelt, J., & de Gier, J. (1982) *Biochim. Biophys. Acta 692*, 126–138.
van Gurp, M., van Heijnsbergen, T., van Ginkel, G., & Levine, Y. K. (1989) *J. Chem. Phys. 90*, 4103–4111.
van Langen, H., Levine, Y. K., Ameloot, M., & Pottel, H. (1987) *Chem. Phys. Lett. 140*, 394–400.
van Langen, H., van Ginkel, G., Shaw, D., & Levine, Y. K. (1989) *Eur. Biophys. J. 17*, 37–48.
Veatch, W. R., & Blout, E. R. (1974) *Biochemistry 13*, 5257–5264.
Vogt, T. C. B., Killian, J. A., Demel, R. A., & de Kruijff, B. (1991) *Biochim. Biophys. Acta 1069*, 525–537.
Wang, S., Beechem, J. M., Gratton, E., & Glaser, M. (1991) *Biochemistry 30*, 5565–5572.
Wallace, B. A. (1990) *Annu. Rev. Biophys. Biophys. Chem. 19*, 127–157.
Watnick, P. I., Chan, S. I., & Dea, P. (1990) *Biochemistry 29*, 6215–6221.
Zannoni, C., Arcioni, A., & Cavatorta, P. (1983) *Chem. Phys. Lipids 32*, 179–250.

BI9420065